Available online at www.sciencedirect.com
ScienceDirect
Tetrahedron
Tetrahedron 63 (2007) 4688–4694

Parvistemins A–D, a new type of dimeric phenylethyl benzoquinones from *Stemona parviflora* Wright

Xinzhou Yang,[a] Tobias A. M. Gulder,[b] Matthias Reichert,[b] Chunping Tang,[a] Changqiang Ke,[a] Yang Ye[a,*] and Gerhard Bringmann[b,*]

[a]*State Key Laboratory of Drug Research, Shanghai Institute of Materia Medica, Chinese Academy of Sciences, 555 Zu-Chong-Zhi Road, Zhangjiang Hightech Park, 201203 Shanghai, PR China*
[b]*Institut für Organische Chemie, Universität Würzburg, Am Hubland, D-97074 Würzburg, Germany*

Received 14 February 2007; revised 12 March 2007; accepted 15 March 2007
Available online 18 March 2007

Dedicated to Professor Lutz F. Tietze on the occasion of his 65th birthday

Abstract—Four naturally occurring dimeric phenylethyl benzoquinones, parvistemins A–D, were isolated from the aerial parts of *Stemona parviflora* Wright. Their constitutions were established by spectroscopic methods. Due to restricted rotation about the central biaryl axis, the compounds are chiral, although racemic. Their two respective atropo-enantiomers were resolved by HPLC on a chiral phase and were stereochemically characterized online, in hyphenation with circular dichroism (CD) spectroscopy (LC–CD coupling), combined with quantum chemical CD calculations.

1. Introduction

The plant species *Stemona parviflora* Wright is distributed in the Hainan province,[1] PR China, only. Its roots have long been used as a substitute for the traditional Chinese medicine 'Baibu',[2,3] against respiratory disorders, including pulmonary tuberculosis and bronchitis, but also against insect pests.[2–4] Previous studies have shown alkaloids to be the main bioactive constituents of this plant.[5–9] As a continuation of our search for new bioactive substances from *S. parviflora*, four novel—axially chiral, yet racemic—dimeric phenylethyl benzoquinones, named parvistemins A–D (**1**–**4**), were isolated from the aerial parts of the plant and their structures were fully established. The analytical resolution of the respective atropo-enantiomers succeeded by chromatography on a chiral HPLC phase. The individual enantiomers were stereochemically analyzed online, right from the peak, by circular dichroism (CD) spectroscopy (LC–CD coupling) and were configurationally assigned using quantum chemical CD calculations.

2. Results and discussion

The ethanol extract of the aerial parts of *S. parviflora* was successively partitioned between water and $CHCl_3$, EtOAc, and *n*-BuOH. The $CHCl_3$-soluble fraction was subjected to Dianion HP-20 resin and Sephadex LH-20 column chromatography to give a brown gum, which was separated by semi-preparative HPLC to yield the parvistemins A–D (**1**–**4**).

In its IR spectrum, parvistemin A (**1**), obtained as an orange-colored amorphous powder, showed hydroxy and carbonyl bands at 3388 and 1648 cm^{-1}, respectively. The characteristic absorption maxima at 268 and 407 nm in the UV spectrum of **1** indicated the presence of a benzoquinone moiety. The HREIMS gave a molecular ion peak at *m*/*z* 482.1736, corresponding to a molecular formula of $C_{30}H_{26}O_6$. Analysis of ^1H and ^{13}C NMR spectra of **1** revealed signals of a monosubstituted benzene ring, a benzoquinone moiety, two methylenes, a methyl, and a hydroxy group (Table 1), with only half the number of ^{13}C atoms (15 instead of 30) and protons (13 instead of 26) expected from the above molecular formula, thus clearly indicating the compound to be a symmetric dimer. The connection of CH_2-8 to the benzene system was evident from the HMBC cross peaks to C-10/C-14. COSY interactions between CH_2-8 and CH_2-7 completed the phenylethyl substructure of **1** (Fig. 1). The constitution of 2-hydroxyl-

Keywords: Benzoquinones; Circular dichroism (CD); Quantum chemical CD calculations; Axial chirality.
* Corresponding authors. Tel.: +49 931 888 5323; fax: +49 931 888 4755; e-mail addresses: bringman@chemie.uni-wuerzburg.de; yye@mail.shcnc.ac.cn

0040–4020/$ - see front matter © 2007 Elsevier Ltd. All rights reserved.
doi:10.1016/j.tet.2007.03.093

Table 1. ^{1}H and ^{13}C NMR data of compounds **1–3** in $CDCl_3$ (δ in ppm, J in Hz)

No.	^{1}H NMR			^{13}C NMR		
	1[a]	**2**[a]	**3**[b]	**1**[c]	**2**[c]	**3**[d]
1,1′				139.6	139.8	139.8
2,2′				185.4	186.4	185.3
3,3′				117.5	117.3	117.2
4,4′				151.2	153.0	151.0
5,5′				182.4	183.1	182.7
6,6′				141.6	142.4	141.8
7,7′	2.61 m, 2.31 m	2.54 m, 2.33 m	2.60 m, 2.37 m	30.3	28.6	28.6
8,8′	2.68 m	2.59 m	2.62 m	34.2	29.8	29.4
9,9′				140.4	127.8	128.7
10,10′	7.07 m			128.2	155.6	157.3
11,11′	7.22 m	6.74 dd (7.2, 1.2)	6.73 br d (8.3)	128.6	115.3	110.3
12,12′	7.17 m	6.95 ddd (7.5, 7.2, 1.5)	7.13 ddd (8.3, 7.3, 1.2)	126.4	127.8	127.7
13,13′	7.22 m	6.66 ddd (7.5, 7.3, 1.2)	6.81 dd (7.8, 7.3)	128.6	119.9	120.6
14,14′	7.07 m	6.98 dd (7.3, 1.5)	6.99 dd (7.8, 1.2)	128.2	130.3	129.9
3,3′-Me	1.96 s	1.96 s	1.91 s	8.2	7.8	8.2
4,4′-OH	6.97 s	6.96 s	6.97 s			
10,10′-OMe			3.62 s			54.9

[a] At 400 MHz.
[b] At 600 MHz.
[c] At 100 MHz.
[d] At 150 MHz.

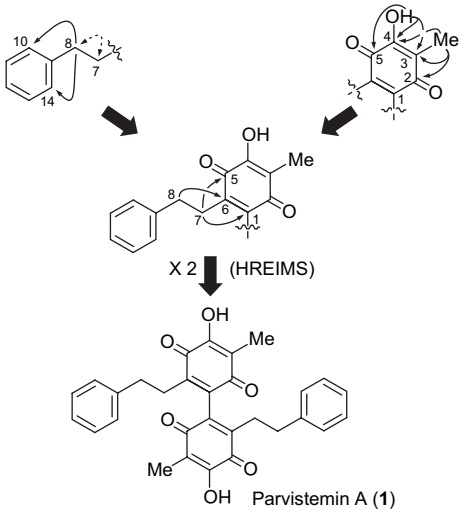

Figure 1. Constitution of parvistemin A (**1**) assembled by using HMBC (full arrows) and COSY (dotted arrow) interactions, and HREIMS data.

3-methyl-benzoquinone moiety was established by HMBC correlations of 4-OH (δ_H 6.97) to C-3, C-4, and C-5, and of 3-methyl (δ_H 1.96) to C-2, C-3, and C-4. The connection between these two molecular portions was established by long-range correlations of CH_2-7 to C-1 and C-5, and of CH_2-8 to C-6, resulting in a phenylethyl 2-hydroxyl-3-methyl-benzoquinone unit ($C_{15}H_{13}O_3$). Considering the molecular formula of **1** ($C_{30}H_{26}O_6$), the reduced number of ^{13}C and ^{1}H signals, and the chemical shift of the quaternary carbon signal at C-1 (δ_C 139.6), compound **1** was found to be a dimer coupled between C-1 and C-1′ as shown in Figure 1.

Parvistemin B (**2**), which was also obtained as an orange-colored powder, gave an HREIMS molecular ion peak at m/z 514.1632, corresponding to the molecular formula $C_{30}H_{26}O_8$. The ^{1}H and ^{13}C NMR spectra of **1** and **2** were almost identical. The observed downfield shift of C-10/C-10′ from 128.2 ppm in **1** to 155.6 ppm in **2** and the increase of the molecular mass by 32 mass units clearly indicated the presence of additional hydroxy groups in these positions. Moreover, the ^{1}H NMR spectrum showed the presence of a 1,2-disubstituted benzene moiety instead of a monosubstituted ring in **1** (Table 1), which again implied that the two hydroxy groups were attached to C-10 and C-10′. This was further confirmed by the long-range correlation of CH_2-8 (8′) (δ_H 2.59) to C-10 (10′), evidencing **2** to possess the structure as displayed in Figure 2.

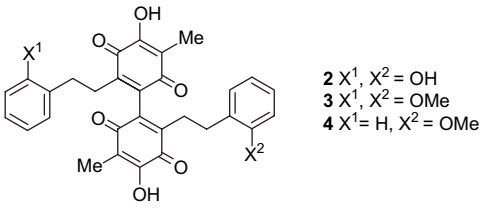

Figure 2. Constitutions of parvistemins B (**2**), C (**3**), and D (**4**).

Parvistemin C (**3**) was isolated as a yellow powder. Its molecular formula was elucidated as $C_{32}H_{30}O_8$ from HREIMS data (542.1934). Comparison of its ^{1}H and ^{13}C NMR data with those obtained for **2** (Table 1) revealed the structural analogy of these metabolites, the only difference being the presence of two methoxy groups at C-10/C-10′ instead of the free hydroxy functions in **2**, which was further confirmed by the ROESY and HMBC data. Therefore, the structure of **3** was established as shown in Figure 2.

Parvistemin D (**4**) was isolated as a brown-yellow powder and its molecular formula was determined as $C_{31}H_{28}O_7$ by HREIMS (512.1834). The ^{1}H NMR spectrum (Table 2) displayed the presence of a monosubstituted benzene,

Table 2. ^{1}H (600 MHz) and ^{13}C NMR (150 MHz) data of **4** in $CDCl_3$ (δ in ppm, J in Hz)

No.	^{1}H NMR	^{13}C NMR	No.	^{1}H NMR	^{13}C NMR
1		139.7	1′		139.5
2		185.1	2′		185.6
3		117.5	3′		117.2
4		151.0	4′		151.3
5		182.4	5′		182.2
6		141.5	6′		142.0
7	2.22 m, 2.64 m	30.3	7′	2.42 m, 2.59 m	28.8
8	2.56 m	34.2	8′	2.66 m	29.4
9		140.7	9′		128.5
10	7.06 br d (7.2)	128.2	10′		157.3
11	7.22 br d (7.6)	128.5	11′	6.67 br d (7.8)	110.3
12	7.16 m	126.3	12′	7.09 ddd (7.8, 7.3, 2.0)	127.8
13	7.22 br d (7.6)	128.5	13′	6.78 dd (7.6, 7.3)	120.6
14	7.06 br d (7.2)	128.2	14′	6.98 dd (7.6, 2.0)	130.0
3-Me	1.91 s	8.2	3′-Me	1.94 s	8.2
4,4′-OH	4.95 s		10′-OMe	3.60 s	54.9

a 1,2-disubstituted benzene, four methylenes, two methyls, and a methoxy function. In this case, the ^{13}C NMR (Table 2) spectrum showed the full set of 31 carbon signals for two aromatic rings, two benzoquinone moieties, four methylenes, two methyls, and a methoxy group. Thus, in contrast to the above symmetric compounds **1**–**3**, parvistemin D (**4**) was identified to be a mixed, non-symmetric hetero-'dimer' built up from a phenylethyl 2-hydroxyl-3-methyl-benzoquinone moiety and a 2-methoxy phenylethyl 2-hydroxyl-3-methyl-benzoquinone portion. The methoxy group (δ_H 3.60) was shown to be located at C-10′ by a ROESY correlation to the respective methylene at δ_H 2.66 (CH_2-8′), resulting in the constitution displayed in Figure 2. The detailed analysis of HSQC and HMBC spectra permitted complete assignment of all ^{1}H and ^{13}C NMR signals (Table 2).

For the investigation of the existence of possible atropo-enantiomers of parvistemin A (**1**) and the determination of their natural ratio, a method for the enantiomeric resolution by HPLC on a chiral phase was developed. Best results were obtained using a Chiralcel OD-H column (Daicel). Interestingly, both the quality and the speed of the separation were increased at elevated temperatures, which even resulted in a perfect baseline separation at 55 °C, with *n*-hexane/isopropanol as the eluents in a 97.5:2.5 ratio. That the two LC–UV peaks observed (Fig. 3a) indeed corresponded to the respective atropo-enantiomers of **1** was verified by online CD analysis (Fig. 3b). Integration of the LC–CD signals obtained gave a 1:1 enantiomeric ratio, demonstrating the fully racemic character of naturally occurring **1**.

For the stereochemical attribution of the two atropo-enantiomers of parvistemin A (**1**), LC–CD spectra were recorded in the stopped-flow mode, providing almost mirror-imaged CD curves. In order to attribute the respective absolute configuration to the corresponding enantiomer of **1**, quantum chemical CD calculations[10] were carried out.

Arbitrarily starting with the *P*-enantiomer, the conformational space of **1** was investigated using at first the semiempirical PM3[11] method. The resulting 40 minimum structures were further optimized by means of DFT (BLYP[12]/6-31G*[13]), thus converging to only two relevant[14] geometries. These two structures were submitted to CD calculations using the OM2[15] Hamiltonian. The single spectra obtained were added following the Boltzmann statistics, resulting in the predicted overall CD curve, which was UV corrected[16] and subsequently compared with the experimental spectra of the faster atropo-enantiomer of **1** (peak A) and the more slowly (peak B) eluting one. These comparisons revealed good agreements between (*P*)-**1** and peak A (Fig. 3c, left) on the one hand, and between (*M*)-**1** and peak B (Fig. 3c, right) on the other, thus permitting assignment of the absolute configurations to the respective enantiomer.

To confirm these attributions, more accurate CD computations using TDDFT (B3LYP[12b,17]/TZVP[18]) were carried out. The resulting CD spectra for (*P*)- and (*M*)-**1** again showed nice agreements between (*P*)-**1** and peak A (Fig. 3d, left) and between (*M*)-**1** and peak B (Fig. 3d, right), thus fully supporting the aforementioned assignment.

For a complete stereochemical attribution of the other—likewise new—isolated secondary metabolites, parvistemins B–D (**2**–**4**), the above-mentioned method for the resolution of the atropo-enantiomers of **1** was individually optimized. In order to achieve the best results, the solvent composition had to be changed to *n*-hexane/isopropanol in a 90:10 ratio for **2** and **3**, and in a 95:5 ratio for **4**. The chromatographic system was tempered to 40 °C in each case, resulting in a baseline separation for the derivatives **2**–**4**, too, thus permitting determination of the racemic nature of all compounds by integration of the LC–UV peaks. For each compound LC–CD spectra were recorded in the stopped-flow mode. Comparison of the online CD spectra of the faster eluting peaks of the parvistemins B–D (**2**–**4**) with the corresponding one in the enantio-separation of **1** revealed the expected high similarity of all these CD curves (Fig. 4), clearly evidencing all faster eluting peaks to correspond to the *P*-configured products.

Previous investigations on the non-alkaloidal constituents of the genus *Stemona* had revealed the existence of stilbenoids, such as stilbostemins B–D (**5**–**7**), which were

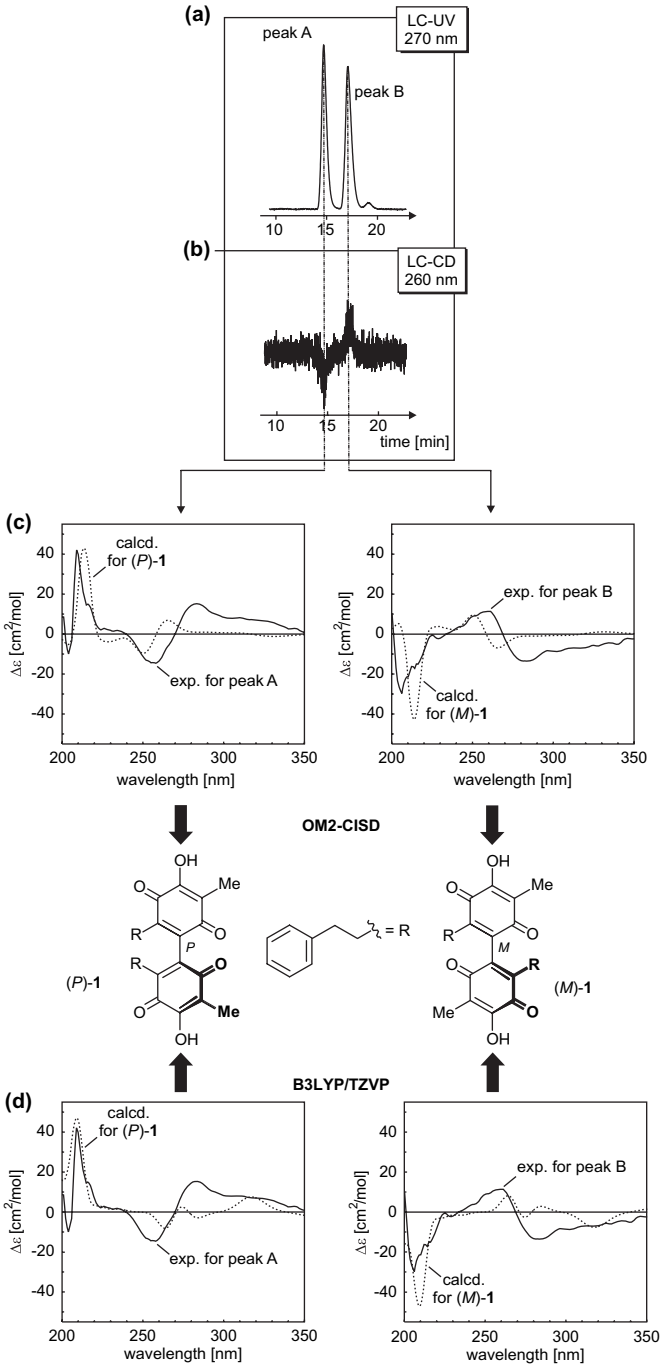

Figure 3. Stereochemical assignment of the two enantiomers of parvistemin A (**1**) by LC–CD coupling and quantum chemical CD calculations using the OM2 Hamiltonian and a TDDFT approach (B3LYP/TZVP).

described for *Stemona tuberosa* Lour,[19] *Stemona collinsae*,[20] and *Stemona* cf. *pierrei*.[21] Taking into account the structural relationship between the new compounds **1**–**4** and the stilbostemins, the latter can be considered as their monomeric biosynthetic precursors. Upon oxygenation of the respective stilbostemin to give **8**, the dimers—either in a symmetric, or in a mixed, non-symmetric form—may be built up by a phenol-oxidative coupling reaction (Scheme 1).[22,23] The possible occurrence of a free, not strongly enzymatically bound radical intermediate **9**, which would attack the respective reaction partner **10** non-stereoselectively from either side, to furnish **11** equally in both enantiomeric forms, may thus explain the formation of the racemic oxidation products **1**–**4**.

There are only a few reports on dimeric stilbenoids from natural sources, which include the dimers of 9,10-dihydrophenanthrenes,[24,25] phenanthrenes,[26,27] and stilbenes,[28–30] but no dimers formed from phenylethyl benzoquinone units. Thus, the parvistemins A–D (**1**–**4**) are the first examples of phenylethyl benzoquinone dimers found in the plant kingdom.

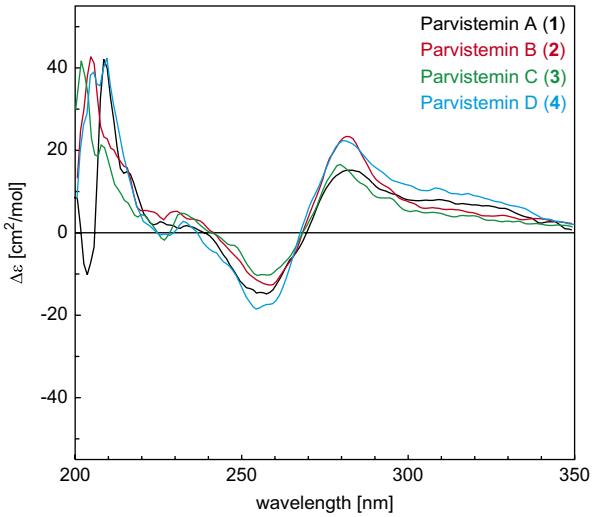

Figure 4. Comparison of the LC–CD spectra of the faster eluting atropo-enantiomers of the parvistemins A–D (**1**–**4**).

on a Nicolet Magna 750 FTIR (KBr) spectrophotometer. Optical rotations were measured on a Perkin–Elmer 341 polarimeter. All MS data were obtained with a Finnigan MAT-95 mass spectrometer. NMR spectra were recorded on a Bruker AM-400 and on a Varian Unity Inova 600 MHz spectrometer with TMS as the internal standard. The chemical shift values are reported in unit (δ) and the coupling constants (J) are given in Hertz. Dianion HP-20 resin [Mitsubishi Chemical (Tokyo, Japan)] and Sephadex LH-20 (25–100 μm, Pharmacia Fine Chemical Co. Ltd.) were used for column chromatography (CC). Semi-preparative HPLC was performed on a Waters 2690 system equipped with a PDA 996 detector (Waters) and a Lichrocart C_{18} column (10 μm, 250×10 mm, Merck). A gradient solvent system from 40% to 80% acetonitrile in water was used at 3.0 mL/min in 30 min. The analytical enantiomeric resolution was performed on a Waters 600 E multisolvent delivery system, Merck-Hitachi L-4000 UV detector, Varian 4290 integrator equipped with a Daicel Chiralcel OD-H column (5 μm, 4.6×250 mm) using a constant flow of 1.2 mL/min.

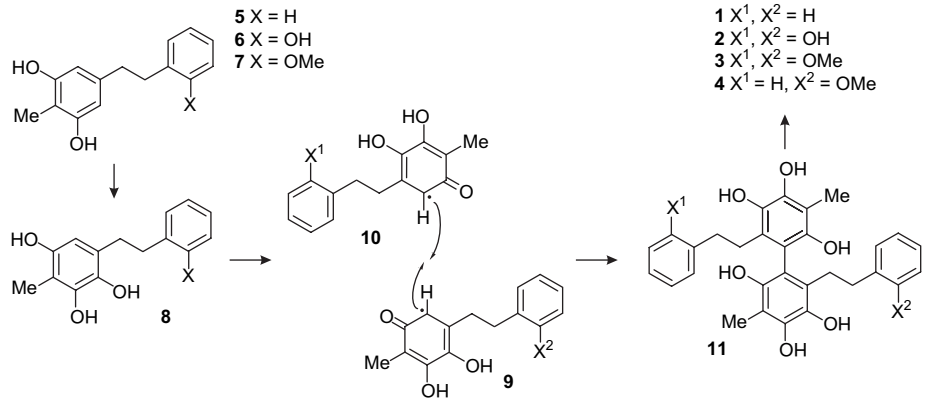

Scheme 1. Proposed biosynthetic pathway to parvistemins A–D (**1**–**4**) by phenol-oxidative coupling of the known stilbostemins B–D (**5**–**7**).

3. Conclusion

In this paper, the first naturally occurring bisphenylethyl benzoquinones are reported. Surprisingly, these axially chiral biquinones are entirely racemic in nature. Still, their atropo-enantiomers were resolved by HPLC on a chiral phase and stereochemically assigned by applying quantum chemical CD calculations.

The occurrence of chiral natural products in a scalemic (i.e., enantiomer-enriched) or even fully racemic form might be unexpected at first glance, but is a well-known phenomenon, in particular in the chemistry of axially chiral natural products.[31] Such a lacking stereoselectivity is explainable by a weak (or even missing) enzymatic assistance and thus lacking stereochemical control in the phenol-oxidative coupling step during the biosynthetic formation of **1**–**4** from their respective monomeric half.

4. Experimental

4.1. General experimental procedures

The UV spectra were taken on a Hewlett-Packard 8452A diode array spectrophotometer. IR spectra were recorded

The chromatographic system was tempered in a Jetstream 2 column oven (Thermotechnic Products GmbH).

4.2. Plant material

The aerial parts of *S. parviflora* were collected in Qiongzhong County, Hainan Province, China, in September, 2003, and identified by Prof. Jin-gui Shen of Shanghai Institute of Materia Medica, Chinese Academy of Sciences. A voucher specimen (20030012B) is deposited in the Herbarium of the institute.

4.3. Extraction and isolation

The dried and chopped aerial parts of *S. parviflora* Wright (1.7 kg) were percolated three times with 95% ethanol (5 L) for 5 days at room temperature. Filtration and evaporation of the solvent of the combined EtOH extracts in vacuo afforded a dark green gum (102.5 g), which was successively partitioned between water and $CHCl_3$, EtOAc, and *n*-BuOH. The $CHCl_3$ fraction (35 g) was absorbed on Dianion HP-20 resin (2 L) and eluted with a gradient of aqueous ethanol. The fraction eluted with EtOH/H_2O=80:20 was subjected to a Sephadex LH-20 column (MeOH/$CHCl_3$=60:40) to give 75 mg of a brown gum, which was submitted to semi-preparative HPLC on a Lichrocart C_{18} column (10 μm,

250×10 mm i.d., Merck) in 7.5 mg portions to give parvistemin A (**1**, t_R 8.7 min, 2.1 mg), parvistemin B (**2**, t_R 11.2 min, 1.0 mg), parvistemin C (**3**, t_R 14.6 min, 0.5 mg), and parvistemin D (**4**, t_R 17.1 min, 0.4 mg) with a gradient solvent system from 40% to 80% acetonitrile as the mobile phase in 30 min.

4.3.1. Parvistemin A (1). Orange-colored amorphous powder; UV (MeOH) λ_{max}: 407, 268, 208 nm; IR (KBr) ν: 3388, 3029, 2925, 1648, 1633, 1600, 1495, 1454, 1394, 1360, 1304, 1166, 1125, 1050, 755, 706, 568 cm^{-1}; HREIMS *m/z* 482.1736 $[M]^+$ (calcd for $C_{30}H_{26}O_6$, 482.1729); EIMS *m/z* (%): 482 $[M]^+$ (62), 391 (49), 377 (34), 373 (16), 335 (8), 287 (15), 272 (6), 105 (23), 91 (100), 83 (26); ^1H and ^{13}C NMR data: see Table 1; ROESY: CH_2-7 (7′)⟷CH_2-8 (8′), CH_2-8 (8′)⟷H-10 (10′), 14 (14′); HMBC (H→C): 3 (3′)-CH_3→2 (2′), 3 (3′), 4 (4′), 4 (4′)-OH→3 (3′), 4 (4′), 5 (5′), CH_2-7 (7′)→1 (1′), 5 (5′), 8 (8′), 9 (9′), CH_2-8 (8′)→6 (6′), 7 (7′), 10 (10′), 14 (14′).

4.3.2. Parvistemin B (2). Orange-colored amorphous powder; UV (MeOH) λ_{max}: 404, 269, 210 nm; IR (KBr) ν: 3405, 2927, 2860, 1654, 1633, 1598, 1506, 1457, 1388, 1297, 1166, 1122, 1097, 1051, 754 cm^{-1}; HREIMS *m/z* 514.1632 $[M]^+$ (calcd for $C_{30}H_{26}O_8$, 514.1628); EIMS *m/z* (%): 514 $[M]^+$ (8), 415 (9), 379 (2), 316 (100), 188 (11), 121 (3), 107 (10); ^1H and ^{13}C NMR data: see Table 1; ROESY: CH_2-7 (7′)⟷CH_2-8 (8′), CH_2-8 (8′)⟷H-10 (10′), 14 (14′); HMBC (H→C): 3 (3′)-CH_3→2 (2′), 3 (3′), 4 (4′), 4 (4′)-OH→3 (3′), 4 (4′), 5 (5′), CH_2-7 (7′)→1 (1′), 5 (5′), 8 (8′), 9 (9′), CH_2-8 (8′)→6 (6′), 7 (7′), 10 (10′), 14 (14′).

4.3.3. Parvistemin C (3). Yellow powder; UV (MeOH) λ_{max}: 410, 272, 200 nm; IR ($CHCl_3$) ν: 3325, 2936, 2855, 2835, 1662, 1636, 1601, 1498, 1462, 1385, 1300, 1163, 1132, 1095, 1054, 760 cm^{-1}; HREIMS *m/z* 542.1934 $[M]^+$ (calcd for $C_{32}H_{30}O_8$, 542.1941); EIMS *m/z* (%): 542 $[M]^+$ (33), 512 (5), 421 (22), 407 (5), 349 (7), 300 (10), 135 (34), 121 (100), 91 (79); ^1H and ^{13}C NMR data: see Table 1; ROESY: CH_2-7 (7′)⟷CH_2-8 (8′), CH_2-8 (8′)⟷10 (10′)-OMe, H-14 (14′), 10 (10′)-OMe⟷H-11 (11′); HMBC (H→C): 3 (3′)-CH_3→2 (2′), 3 (3′), 4 (4′), 4 (4′)-OH→3 (3′), 4 (4′), 5 (5′), CH_2-7 (7′)→1 (1′), 5 (5′), 8 (8′), 9 (9′), CH_2-8 (8′)→6 (6′), 7 (7′), 10 (10′), 14 (14′), 10 (10′)-OMe→10 (10′).

4.3.4. Parvistemin D (4). Brown-yellow powder; UV (MeOH) λ_{max}: 406, 269, 198 nm; IR ($CHCl_3$) ν: 3398, 2932, 2853, 1656, 1635, 1604, 1497, 1455, 1379, 1300, 1162, 1127, 1089, 1048, 727 cm^{-1}; HREIMS *m/z* 512.1834 $[M]^+$ (calcd for $C_{31}H_{28}O_7$, 512.1835); EIMS *m/z* (%): 512 $[M]^+$ (78), 391 (39), 319 (7), 135 (12), 121 (94), 91 (100); ^1H and ^{13}C NMR data: see Table 2; ROESY: CH_2-7 (7′)⟷CH_2-8 (8′), CH_2-8⟷H-10, 14, CH_2-8′⟷10′-OMe, H-14′, 10′-OMe⟷H-11′; HMBC (H→C): 3 (3′)-CH_3→2 (2′), 3 (3′), 4 (4′), 4 (4′)-OH→3 (3′), 4 (4′), 5 (5′), CH_2-7 (7′)→1 (1′), 5 (5′), 8 (8′), 9 (9′), C_2H-8 (8′)→6 (6′), 7 (7′), 10 (10′), 14 (14′), 10′-OMe→10′.

4.4. Computational

The conformational analysis of **1** was performed by means of the semiempirical PM3[11] method and a DFT approach (BLYP[12]/6-31G*[13]), as implemented in the program package GAUSSIAN 03,[32] starting from preoptimized geometries generated by the TRIPOS[33] force field as part of the molecular modeling package SYBYL 7.2.[33] The wave functions required for the computation of the respective oscillator and rotational strengths of the electronic transitions from the ground state to excited states were obtained by OM2[15] calculations followed by CISD computations including each 400 singly and doubly occupied configurations, as well as the ground state determinant, using the MNDO99[34] software package. Furthermore, the oscillator and rotatory strengths for the first 100 transitions were calculated by means of TDDFT using the B3LYP[12b,17] hybrid functional and a TZVP[18] basis set as implemented in TURBOMOLE 5.6.[35] The oscillator and rotatory strengths, thus obtained for the individual geometries, were summed energetically weighted, following the Boltzmann statistics. Finally, the overall UV and CD spectra were simulated as sums of Gaussian functions centered at the wavelengths of the respective electronic transitions and multiplied by the corresponding oscillator or rotatory strengths—transformed into absorption and $\Delta\varepsilon$ values, respectively.

Acknowledgements

This work was supported by the National Natural Science Foundation of China (Grant no. 30123005), the Science and Technology Committee of Shanghai, PR China (no. 036505003), the Fonds der Chemischen Industrie (supplies to G.B.), and the DFG (SFB 630 and SPP 1152).

References and notes

1. Guangdong Institute of Botany. *Flora of Hainan*; Sciences: Beijing, PR China, 1977; Vol. 4, p 148.
2. Jiangsu New Medical College. *The Dictionary of Traditional Chinese Medicine*; Shanghai Science and Technology Press: Shanghai, PR China, 1986; p 860.
3. Xu, G. J.; He, H. X.; Xu, L. S.; Jin, R. Y. *The Chinese Materia Medica (Zhonghua Benchao)*; Chinese Medicinal Science and Technology Publishing House: Beijing, PR China, 1996; pp 467–472.
4. Sakata, K.; Aoki, K.; Chang, C. F.; Sakurai, A. *Agric. Biol. Chem.* **1978**, *42*, 457–463.
5. Lin, W. H.; Xu, R. S.; Zhong, Q. X. *Acta Chim. Sin.* **1990**, *48*, 811–814.
6. Lin, W. H.; Xu, R. S.; Zhong, Q. X. *Acta Chim. Sin.* **1991**, *49*, 927–931.
7. Lin, W. H.; Xu, R. S.; Zhong, Q. X. *Acta Chim. Sin.* **1991**, *49*, 1034–1037.
8. Ke, C. Q.; He, Z. S.; Yang, Y. P.; Ye, Y. *Chin. Chem. Lett.* **2003**, *14*, 173–175.
9. Pilli, R. A.; Oliveria, M. C. F. *Nat. Prod. Rep.* **2000**, *17*, 117–127.
10. (a) Bringmann, G.; Gulder, T.; Reichert, M.; Meyer, F. *Org. Lett.* **2006**, *8*, 1037–1040; (b) Wanjohi, J. M.; Yenesew, A.; Midiwo, J. O.; Heydenreich, M.; Peter, M. G.; Dreyer, M.; Reichert, M.; Bringmann, G. *Tetrahedron* **2005**, *61*, 2667–2674; (c) Bringmann, G.; Mühlbacher, J.; Reichert, M.; Dreyer, M.; Kolz, J.; Speicher, A. *J. Am. Chem. Soc.* **2004**, *126*, 9283–9290.
11. Stewart, J. J. P. *J. Comput. Chem.* **1989**, *10*, 209–264.

12. (a) Becke, A. D. *Phys. Rev. A* **1988**, *38*, 3098–3100; (b) Lee, C.; Yang, W.; Parr, R. G. *Phys. Rev. B* **1988**, *37*, 785–789.
13. Hariharan, P. C.; Pople, J. A. *Theor. Chim. Acta* **1973**, *28*, 213–222.
14. The CD spectra of those structures that lie energetically higher than 3 kcal/mol above the global minimum found, do not significantly contribute to the overall CD curve.
15. Weber, W.; Thiel, W. *Theor. Chem. Acc.* **2000**, *103*, 495–506.
16. Bringmann, G.; Busemann, S. *Natural Product Analysis*; Schreier, P., Herderich, M., Humpf, H. U., Schwab, W., Eds.; Vieweg: Wiesbaden, 1998; pp 195–212.
17. Becke, A. D. *J. Chem. Phys.* **1993**, *98*, 5648–5652.
18. Schäfer, A.; Huber, C.; Ahlrichs, R. *J. Chem. Phys.* **1994**, *100*, 5829–5835.
19. Zhao, W. M.; Qin, G. W.; Ye, Y.; Xu, R. S.; Le, X. F. *Phytochemistry* **1995**, *38*, 711–713.
20. Pacher, T.; Seger, C.; Engelmeier, D.; Vajrodaya, S.; Hofer, O.; Greger, H. *J. Nat. Prod.* **2002**, *65*, 820–827.
21. Kostecki, K.; Engelmeier, D.; Paucher, T.; Hofer, O.; Vajrodaya, S.; Greger, H. *Phytochemistry* **2004**, *65*, 99–106.
22. Baxter, I.; Titman, R. B. *J. Chem. Soc. C* **1970**, 2078–2082.
23. Corbett, J. F. *J. Chem. Soc. C* **1967**, 611–620.
24. Lin, Y. L.; Chen, W. P.; Macabalang, A. D. *Chem. Pharm. Bull.* **2005**, *53*, 1111–1113.
25. Li, B.; Masae, Y.; Keiko, I.; Shuzo, T. *Phytochemistry* **1990**, *29*, 1259–1260.
26. Li, B.; Tomoko, K.; Keiko, I.; Masae, Y.; Shuzo, T. *Phytochemistry* **1991**, *30*, 2733–2735.
27. Masae, Y.; Li, B.; Tomoko, K.; Keiko, I.; Shuzo, T.; Yuriko, Y.; Kenichi, T. *Phytochemistry* **1992**, *31*, 3985–3987.
28. Iliya, I.; Ali, Z.; Tanaka, T.; Iinuma, M.; Furusawa, M.; Nakaya, K.; Murata, J.; Darnaedi, D.; Matsuura, N.; Ubukata, M. *Phytochemistry* **2003**, *62*, 601–606.
29. Li, X. M.; Lin, M.; Wang, Y. H. *J. Asian Nat. Prod. Res.* **2003**, *5*, 113–119.
30. Tanaka, T.; Iliya, I.; Ito, T.; Furusawa, M.; Nakaya, K. I.; Iinuma, M.; Shirataki, Y.; Matsuura, N.; Ubukata, M.; Murata, J.; Simozono, F.; Hirai, K. *Chem. Pharm. Bull.* **2001**, *49*, 858–862.
31. (a) Cass, Q. B.; Tiritan, E.; Matlin, S. A.; Freire, E. C. *Phytochemistry* **1991**, *30*, 2655–2657; (b) Bringmann, G.; Tasler, S.; Endress, H.; Kraus, J.; Messer, K.; Wohlfarth, M.; Lobin, W. *J. Am. Chem. Soc.* **2001**, *123*, 2703–2711; (c) Bringmann, G.; Günther, C.; Ochse, M.; Schupp, O.; Tasler, S. *Progr. Chem. Org. Nat. Prod.*; Herz, W., Falk, H., Kirby, G. W., Moore, R. E., Tamm, C., Eds.; Springer: Wien, 2001; Vol. 82, pp 1–249.
32. Frisch, M. J.; Trucks, G. W.; Schlegel, H. B.; Scuseria, G. E.; Robb, M. A.; Cheeseman, J. R.; Montgomery, J. A., Jr.; Vreven, T.; Kudin, K. N.; Burant, J. C.; Millam, J. M.; Iyengar, S. S.; Tomasi, J.; Barone, V.; Mennucci, B.; Cossi, M.; Scalmani, G.; Rega, N.; Petersson, G. A.; Nakatsuji, H.; Hada, M.; Ehara, M.; Toyota, K.; Fukuda, R.; Hasegawa, J.; Ishida, M.; Nakajima, T.; Honda, Y.; Kitao, O.; Nakai, H.; Klene, M.; Li, X.; Knox, J. E.; Hratchian, H. P.; Cross, J. B.; Adamo, C.; Jaramillo, J.; Gomperts, R.; Stratmann, R. E.; Yazyev, O.; Austin, A. J.; Cammi, R.; Pomelli, C.; Ochterski, J. W.; Ayala, P. Y.; Morokuma, K.; Voth, G. A.; Salvador, P.; Dannenberg, J. J.; Zakrzewski, V. G.; Dapprich, S.; Daniels, A. D.; Strain, M. C.; Farkas, O.; Malick, D. K.; Rabuck, A. D.; Raghavachari, K.; Foresman, J. B.; Ortiz, J. V.; Cui, Q.; Baboul, A. G.; Clifford, S.; Cioslowski, J.; Stefanov, B. B.; Liu, G.; Liashenko, A.; Piskorz, P.; Komaromi, I.; Martin, R. L.; Fox, D. J.; Keith, T.; Al-Laham, M. A.; Peng, C. Y.; Nanayakkara, A.; Challacombe, M.; Gill, P. M. W.; Johnson, B.; Chen, W.; Wong, M. W.; Gonzalez, C.; Pople, J. A. *GAUSSIAN 03, Revision B.04*; Gaussian: Pittsburgh, PA, 2003.
33. *SYBYL 7.2*; Tripos: St. Louis, MO, 2006.
34. Tiehl, W. *MNDO99, Version 6.0*; Max-Planck-Institut für Kohlenforschung: Mühlheim, Germany, 2001.
35. Ahlrichs, R.; Bär, M.; Baron, H.-P.; Bauerschmitt, R.; Böcker, S.; Deglmann, P.; Ehrig, M.; Eichkorn, K.; Elliott, S.; Furche, F.; Haase, F.; Häser, M.; Horn, H.; Hättig, C.; Huber, C.; Huniar, U.; Kattannek, M.; Köhn, A.; Kölmel, C.; Kollwitz, M.; May, K.; Ochsenfeld, C.; Öhm, H.; Patzelt, H.; Rubner, O.; Schäfer, A.; Schneider, U.; Sierka, M.; Treutler, O.; Unterreiner, B.; Arnim, M. V.; Weigend, F.; Weis, P.; Weiss, H. *TURBOMOLE, Version 5.6*; Universität Karlsruhe: Karlsruhe, Germany, 2002.